Національна академія наук України

ІНСТИТУТ ФІЗИКИ КОНДЕНСОВАНИХ СИСТЕМ

ICMP–15–14E

I.S. Bzovska, I.M. Mryglod

SPATIOTEMPORAL PATTERN FORMATION IN CO OXIDATION REACTION. THE ROLE OF DIFFUSION

ЛЬВІВ

УДК: 538.9

PACS: 82.40.Bj, 82.45.Jn

Формування просторово-часових структур в реакції окислення монооксиду вуглецю. Роль дифузії

І.С. Бзовська, І.М. Мриглод

Анотація. Досліджуються механізми формування просторово-часових структур у каталітичній реакції окислення CO з урахуванням процесів дифузії на неоднорідній поверхні Pt(110), яка містить структурно відмінні ділянки, що утворюються під час CO-індукованого переходу від реконструйованої 1×2 фази до об'ємної 1×1 фази. Показано, що система може втрачати стійкість двома шляхами: або через біфуркацію Хопфа, що веде до утворення в системі часових структур – автоколивань, або через біфуркацію Тюринга, що призводить до формування регулярних просторових структур. При одночасній реалізації обох сценаріїв у системі спостерігаються просторово-часові структури для величини покриття θ_{O}. Розподіл θ_{CO} залишається практично однорідним у просторі та незалежним від геометрії поверхні.

Spatiotemporal pattern formation in CO oxidation reaction. The role of diffusion

I.S. Bzovska, I.M. Mryglod

Abstract. The spatiotemporal pattern formation in the catalytic carbon monoxide oxidation reaction with taking into account the diffusion processes over the Pt(110) surface, which may contain structurally different areas, is studied. These areas are formed during CO-induced transition from a reconstructed phase with 1×2 geometry of the overlayer to a bulk-like (1×1) phase with square atomic arrangement. It is shown that the system may lose its stability in two ways – either through the Hopf bifurcation leading to the formation of temporal patterns in the system, namely oscillations, or through the Turing bifurcation leading to the formation of regular spatial patterns. At simultaneous implementation of both scenarios spatiotemporal patterns for oxygen coverage θ_{O} are observed in the system. The distribution of θ_{CO} is almost homogeneous in space and independent of the surface geometry.

Препринти Інституту фізики конденсованих систем НАН України розповсюджуються серед наукових та інформаційних установ. Вони також доступні по електронній комп'ютерній мережі на WWW-сервері інституту за адресою http://www.icmp.lviv.ua/

The preprints of the Institute for Condensed Matter Physics of the National Academy of Sciences of Ukraine are distributed to scientific and informational institutions. They also are available by computer network from Institute's WWW server (http://www.icmp.lviv.ua/)

Ірина Степанівна Бзовська
Ігор Миронович Мриглод

Просторово-часові структури в реакції окислення монооксиду вуглецю. Роль дифузії

Роботу отримано 28 грудня 2015 р.

Затверджено до друку Вченою радою ІФКС НАН України

Рекомендовано до друку семінаром відділу квантово-статистичної теорії процесів каталізу

Виготовлено при ІФКС НАН України

Introduction

In recent times, spatiotemporal pattern formation in spatially extended systems, such as reaction-diffusion systems, has been extensively studied [1–4]. In these systems the concentration of one or more substances distributed in space can change under the influence of two processes: local chemical reactions in which the substances are transformed into each other, and diffusion which causes the substances to spread out over a surface in space.

Among chemical systems, the catalytic oxidation of CO on platinum (110) is one of the most prominent examples of a reaction-diffusion system showing a variety of complex spatiotemporal patterns [5–8]. For this system various experiments on pattern formation have been carried out. Pattern formation was monitored by means of photoemission electron microscopy (PEEM) [9–11]. The experimental parameters were chosen such that the reaction was oscillatory and, furthermore, uniform oscillations were unstable and a complex state of spiral-wave turbulence spontaneously developed.

An orientation of the catalyst surface in such systems has a decisive influence on the occurrence of oscillations and surface patterns [3, 5, 6]. The clean Pt(110) top surface layer reconstructs into a 1×2 "missing row" structure. This reconstruction can be reversibly lifted by adsorption of CO molecules. Because oxygen adsorption is favored on the unreconstructed 1×1 phase, periodic switching between two states of different catalytic activity can occur, resulting in temporal oscillations of the reaction rate. Local spatial coupling across the catalytic surface is provided by surface diffusion of adsorbed CO and oxygen. Under such oscillatory conditions, the interplay between reaction and diffusion processes can lead to the development of spatiotemporal patterns.

Formation of spatiotemporal patterns occurs under two main symmetry-breaking instabilities as the Hopf and the Turing ones [12,13]. An interaction and competition of these bifurcations have been considered for different reaction-diffusion systems, including Belousov-Zhabotinsky autocatalytic reaction [14], the FitzHugh-Nagumo model [12, 13], etc. In these models a variety of modes has been received, including mixed modes – spatial patterns modulated in time.

In this paper we study the mechanism of spatiotemporal pattern formation in the carbon monoxide oxidation reaction on the surface of Pt(110). A simple three-variable model has been developed to account for most of the dynamic features of the reaction. Analysis of instabilities in time and space of the system is based on methods of linear stability

theory and numerical modelling. It is shown that under certain values of parameters in the system there are patterns provided by linear analysis and similar to those observed in the experiment.

The paper is organized as follows. A model of the catalytic oxidation reaction of carbon monoxide and the linear stability theory are introduced in the following section. In Sec. III, the results of our calculations and a discussion of the obtained results are shown. Cases of homogeneous and inhomogeneous surfaces are described in detail. The paper ends with conclusions in Sec. IV.

1. Model and theory

Let us consider a model of the catalytic oxidation reaction of carbon monoxide that takes the diffusion processes over the Pt(110) surface into account. For this, diffusion terms were included into the system of kinetic differential equations describing the dynamic behavior of the model [15, 16]:

$$\frac{\mathrm{d}\theta_{\mathrm{CO}}}{\mathrm{d}\tau} = D_1\triangle\theta_{\mathrm{CO}} + p_{\mathrm{CO}}k_{\mathrm{CO}}s_{\mathrm{CO}}(1-\theta_{\mathrm{CO}}^q) - d\theta_{\mathrm{CO}} - k_r\theta_{\mathrm{CO}}\theta_{\mathrm{O}}, \quad (1)$$

$$\frac{\mathrm{d}\theta_{\mathrm{O}}}{\mathrm{d}\tau} = D_2\triangle\theta_{\mathrm{O}} + p_{\mathrm{O}_2}k_{\mathrm{O}}(s_{1\times1}\theta_{1\times1} + s_{1\times2}(1-\theta_{1\times1})) \times (1-\theta_{\mathrm{CO}}-\theta_{\mathrm{O}})^2 - k_r\theta_{\mathrm{CO}}\theta_{\mathrm{O}}, \quad (2)$$

$$\frac{\mathrm{d}\theta_{1\times1}}{\mathrm{d}\tau} = D_3\triangle\theta_{1\times1} + k_5\left(\left[1+\exp\left(\frac{u_0-\theta_{\mathrm{CO}}}{\delta u}\right)\right]^{-1} - \theta_{1\times1}\right). \quad (3)$$

Equation (1) describes the change in the number of adsorbed CO with taking into account the chemical reaction with adsorbed oxygen, desorption of CO with desorption constant d and diffusion of CO. Equation (2) describes the diffusion of oxygen, its dissociative adsorption and changes due to CO oxidation reaction. Equation (3) is the kinetic equation for the surface transformation. Function $\left[1+\exp\left(\frac{u_0-\theta_{\mathrm{CO}}}{\delta u}\right)\right]^{-1}$ is a non-decreasing and smooth function of θ_{CO} at the interval [0,1], which allows us to describe the transformation of the reconstructed 1×2 surface structure to the 1×1 structure depending on the amount of CO coverage [6]. For an inhomogeneous surface, the laplacian term $\triangle\theta_{1\times1}$ in equation (3) originates from the contribution of the interfaces between different surface geometries to the total system energy [8]. Consequently, the coefficient D_3 describes the energy costs of such interfaces. In this model

the precursor-type kinetics of CO adsorption is accounted for by the exponent $q = 3$ in the right hand of equation (1). It makes the model more realistic since the inhibition of adsorption of CO and O_2 is asymmetric and preadsorbed CO blocks oxygen adsorption but not vice versa. A more detailed explanation and values of the parameters used in further calculations are presented in Table 1 [6].

Table 1. Parameters of the model

T	540 K	Temperature
p_{O_2}	9.75×10^{-5} Torr	O_2 partial pressure
k_{CO}	4.2×10^{5} s^{-1}Torr^{-1}	Impingement rate of CO
k_{O}	7.8×10^{5} s^{-1}Torr^{-1}	Impingement rate of O_2
d	10.21 s^{-1}	CO desorption rate
D_1	10^{-7} cm^{2}s^{-1}	CO diffusion rate
D_2	10^{-10} cm^{2}s^{-1}	O diffusion rate
k_r	283.8 s^{-1}	Reaction rate
s_{CO}	1	CO sticking coefficient
$s_{\mathrm{O},1\times2}$	0.4	Oxygen sticking coefficient on the 1×2 phase
u_0, δu	0.35, 0.05	Parameters for the structural phase transition
k_5	1.61 s^{-1}	Phase transition rate

System (1)–(3) can be transformed by the substitution

$$t = k_r\tau, \quad \overline{D}_{1,2,3} = D_{1,2,3}/k_r, \quad \overline{p}_{\mathrm{CO}} = p_{\mathrm{CO}}k_{\mathrm{CO}}s_{\mathrm{CO}}/k_r,$$
$$\overline{p}_{\mathrm{O}_2} = p_{\mathrm{O}_2}k_{\mathrm{O}}s_{\mathrm{O}}^{1\times2}/k_r, \quad \overline{d} = d/k_r, \quad \overline{k}_5 = k_5/k_r$$

into the following dimensionless form:

$$\frac{\mathrm{d}\theta_{\mathrm{CO}}}{\mathrm{d}t} = F_1(\theta_{\mathrm{CO}},\theta_{\mathrm{O}}) = \overline{D}_1\triangle\theta_{\mathrm{CO}} + \overline{p}_{\mathrm{CO}}(1-\theta_{\mathrm{CO}}^3) - \overline{d}\theta_{\mathrm{CO}} - \theta_{\mathrm{CO}}\theta_{\mathrm{O}}, \quad (4)$$

$$\frac{\mathrm{d}\theta_{\mathrm{O}}}{\mathrm{d}t} = F_2(\theta_{\mathrm{CO}},\theta_{\mathrm{O}},\theta_{1\times1}) = \overline{D}_2\triangle\theta_{\mathrm{O}} + \overline{p}_{\mathrm{O}_2}(1+\theta_{1\times1})(1-\theta_{\mathrm{CO}}-\theta_{\mathrm{O}})^2 - \theta_{\mathrm{CO}}\theta_{\mathrm{O}}, \quad (5)$$

$$\frac{\mathrm{d}\theta_{1\times1}}{\mathrm{d}t} = F_3(\theta_{\mathrm{CO}},\theta_{1\times1}) = \overline{D}_3\triangle\theta_{1\times1} + \overline{k}_5\left(\left[1+\exp\left(\frac{u_0-\theta_{\mathrm{CO}}}{\delta u}\right)\right]^{-1} - \theta_{1\times1}\right). \quad (6)$$

$s_{\mathrm{O}} = s_{\mathrm{O}}^{1\times1}\theta_{1\times1} + s_{\mathrm{O}}^{1\times2}(1-\theta_{1\times1}) = s_{\mathrm{O}}^{1\times2}(1+\theta_{1\times1})$ under the assumption that for Pt(110) we have $s_{\mathrm{O}}^{1\times1}/s_{\mathrm{O}}^{1\times2} \simeq 2$.

The system of differential equations (4) – (6) with partial derivatives can not be solved analytically. Therefore, analysis of the system instabilities in time and space has been based on methods of the linear stability theory and numerical simulations. The system of equations (4)–(6) in the linear approximation for the deviations from steady state $\delta\theta_i(\mathbf{r},t) = \theta_i(\mathbf{r},t) - \theta_{i,s}(\mathbf{r})$ looks like

$$\frac{\partial}{\partial t}\delta\theta_i(\mathbf{r},t) = \sum_{j=1}^{3}\left(\frac{\partial F_i}{\partial\theta_j}\right)_{\theta_k=\theta_{k,s}}\delta\theta_j(\mathbf{r},t) + \overline{D}_i\triangle\delta\theta_i(\mathbf{r},t), \qquad (7)$$
$$i,j = \mathrm{CO},\mathrm{O},1\times 1.$$

Stability of the system has been investigated using the method of normal modes concerning periodic in space perturbation (normal mode) with the wavelength λ. For this, we do the following substitution $\delta\theta_i(\mathbf{r},t) \sim \mathrm{e}^{\omega t + i\mathbf{kr}}$, where $k = 2\pi/\lambda$ is a wave number, and we obtain the following linear system of equations

$$\sum_{j=1}^{3}\left[\left(\frac{\partial F_i}{\partial\theta_j}\right)_{\theta_k=\theta_{k,s}} - \overline{D}_i k^2\delta_{ij} - \omega\delta_{ij}\right]\delta\theta_j = 0, \quad i = 1,2,3. \qquad (8)$$

Stability analysis requires the solution of the secular equation

$$\det\left\|\left(\frac{\partial F_i}{\partial\theta_j}\right)_{\theta_k=\theta_{k,s}} - \overline{D}_i k^2\delta_{ij} - \omega\delta_{ij}\right\| = 0, \qquad (9)$$

from there we get an equation for $\omega(k)$:

$$\omega^3 - b(k)\omega^2 + c(k)\omega - d(k) = 0, \qquad (10)$$

where we have introduced the next notations:

$$\begin{aligned}
b(k) &= \sigma - k^2(\overline{D}_1 + \overline{D}_2 + \overline{D}_3),\\
c(k) &= \Sigma - k^2[\overline{D}_1(a_{22}+a_{33}) + \overline{D}_2(a_{11}+a_{33}) + \overline{D}_3(a_{11}+a_{22})]\\
&+ k^4(\overline{D}_1\overline{D}_2 + \overline{D}_1\overline{D}_3 + \overline{D}_2\overline{D}_3),\\
d(k) &= \Delta - k^2\sum_{i=1}^{3}\overline{D}_i\eta_i + k^4(a_{11}\overline{D}_2\overline{D}_3 + a_{22}\overline{D}_1\overline{D}_3 + a_{33}\overline{D}_1\overline{D}_2)\\
&- k^6\overline{D}_1\overline{D}_2\overline{D}_3.
\end{aligned}$$

Here $a_{ij} = \left(\frac{\partial F_i}{\partial\theta_j}\right)_{\theta_k=\theta_{k,s}}$, $\sigma = a_{11}+a_{22}+a_{33}$ is the trace of the characteristic matrix $\{a_{ij}\}$, $\Delta = a_{11}(a_{22}a_{33} - a_{23}a_{32}) - a_{12}(a_{21}a_{33} - a_{23}a_{31}) + a_{13}(a_{21}a_{32} - a_{22}a_{31})$ is its determinant, $\Sigma = \sum_{i=1}^{3}\eta_i$, where $\eta_i = a_{jj}a_{ll} - a_{jl}a_{lj}$, $i \neq j \neq l$. For our model

$$\begin{aligned}
a_{11} &= -3\overline{p}_{\mathrm{CO}}\theta_{\mathrm{CO},s}^2 - \overline{d} - \theta_{\mathrm{O},s}, \quad a_{12} = -\theta_{\mathrm{CO},s}, \quad a_{13} = 0,\\
a_{21} &= -2\overline{p}_{\mathrm{O}_2}(1+\theta_{1\times1,s})(1-\theta_{\mathrm{CO},s}-\theta_{\mathrm{O},s}) - \theta_{\mathrm{O},s},\\
a_{22} &= -2\overline{p}_{\mathrm{O}_2}(1+\theta_{1\times1,s})(1-\theta_{\mathrm{CO},s}-\theta_{\mathrm{O},s}) - \theta_{\mathrm{CO},s},\\
a_{23} &= \overline{p}_{\mathrm{O}_2}(1-\theta_{\mathrm{CO},s}-\theta_{\mathrm{O},s})^2, \qquad (11)\\
a_{31} &= \frac{\overline{k}_5}{\delta u}\frac{\exp\left(\dfrac{u_0-\theta_{\mathrm{CO},s}}{\delta u}\right)}{\left[1+\exp\left(\dfrac{u_0-\theta_{\mathrm{CO},s}}{\delta u}\right)\right]^2}, \quad a_{32} = 0, \quad a_{33} = -\overline{k}_5.
\end{aligned}$$

Equation (10) is a cubic equation with real coefficients. The solutions of (10) are

$$\omega_{1,2,3}(k) = \sqrt[3]{-\frac{q(k)}{2} + \sqrt{D(k)}} + \sqrt[3]{-\frac{q(k)}{2} - \sqrt{D(k)}} + \frac{b(k)}{3}, \qquad (12)$$

where the following notations were introduced for the convenience:

$$\begin{aligned}
q(k) &= -\frac{2b^3(k)}{27} + \frac{b(k)c(k)}{3} - d(k),\\
p(k) &= c(k) - \frac{b^2(k)}{3},\\
D(k) &= \frac{q^2(k)}{4} + \frac{p^3(k)}{27}.
\end{aligned}$$

Equation (12) is the dispersion relation which in general can contain both real and imaginary parts, i.e. $\omega(k) = \mathrm{Re}\,\omega(k) + i\mathrm{Im}\,\omega(k)$. The component $\mathrm{Re}\,\omega(k)$ describes the stability of a solution ($\delta\theta_{\mathrm{CO},k}(\omega)$, $\delta\theta_{\mathrm{O},k}(\omega)$, $\delta\theta_{1\times1,k}(\omega)$) and defines the process of relaxation, while $\mathrm{Im}\,\omega(k)$ sets the frequency of the oscillating process.

Let's consider cubic equation (10) in more detail. Assume that $\omega_1, \omega_2, \omega_3$ are its solutions. It is well-known that coefficients of a cubic equation and its roots are connected by the relations:

$$\begin{aligned}
b &= \omega_1 + \omega_2 + \omega_3,\\
c &= \omega_1\omega_2 + \omega_1\omega_3 + \omega_2\omega_3, \qquad (13)\\
d &= \omega_1\omega_2\omega_3,\\
bc - d &= (\omega_1+\omega_2)(\omega_1+\omega_3)(\omega_2+\omega_3).
\end{aligned}$$

The investigated state is stable if for all eigenvalues of characteristic equation (9)

$$\mathrm{Re}\,\omega_i(k) < 0, \qquad i = 1, 2, 3. \tag{14}$$

Consequently, as follows from relations (13) and (14), the homogeneous state of the whole system is stable when

$$\begin{aligned} b &< 0, \\ c &> 0, \\ d &< 0, \\ bc - d &< 0. \end{aligned} \tag{15}$$

The homogeneous state of the system becomes unstable when at least for one $\omega_i(k)$ $(i = 1, 2, 3)$ $\mathrm{Re}\,\omega_i(k) > 0$. The violation of any of inequalities (15) means that in the system a bifurcation has occurred. The broken condition $d<0$ means the appearance of one real positive eigenvalue in the system. The broken condition $bc-d < 0$ means there are two complex conjugate eigenvalues with positive real part. The first case corresponds to the Turing bifurcation, and the second – to the Hopf one.

In [17] authors represent the function $d(k)$ as $d(k^2) = \Delta - \alpha_T k^2 + \beta_T k^4 - \delta_T k^6$, where $\alpha_T = \sum_{i=1}^{3} \overline{D}_i \eta_i$, $\beta_T = a_{11}\overline{D}_2\overline{D}_3 + a_{22}\overline{D}_1\overline{D}_3 + a_{33}\overline{D}_1\overline{D}_2$, $\delta_T = \overline{D}_1\overline{D}_2\overline{D}_3$. Function $d(k^2)$ is a cubic parabola which has local extremes. The maximum is

$$d_{\max}(k_T^2) = \Delta + \frac{1}{27\delta_T^2}\left[2(\beta_T^2 - 3\alpha_T\delta_T)^{\frac{3}{2}} + \beta_T(2\beta_T^2 - 9\alpha_T\delta_T)\right] \tag{16}$$

and is reached at the point $k_T^2 = (\beta_T + \sqrt{\beta_T^2 - 3\alpha_T\delta_T})/3\delta_T^2$. For the Turing bifurcation it is necessary that in a certain range of wave numbers $d(k^2)$ has become greater than zero, $d_{\max}(k_T^2) > 0$. As the authors affirm, it is only possible if at least one of the coefficients on the main diagonal of matrix $\{a_{ij}\}$ is greater than zero (a well-known condition for the existence of autocatalysis).

The condition for the Hopf bifurcation is obtained in [17] in the similar way and is

$$\begin{aligned} &k_0^2 = (\beta_V + \sqrt{\beta_V^2 - 3\alpha_V\delta_V})/3\delta_V^2, \\ &F_{\max}(k_0^2) = bc - d = \sigma\Sigma - \Delta \\ &+\frac{1}{27\delta_V^2}\left[2(\beta_V^2 - 3\alpha_V\delta_V)^{\frac{3}{2}} + \beta_V(2\beta_V^2 - 9\alpha_V\delta_V)\right] > 0. \end{aligned} \tag{17}$$

Here

$$\begin{aligned} \alpha_V &= \overline{D}_1(\sigma^2 - a_{11}^2 - a_{13}a_{31} - a_{12}a_{21}) + \overline{D}_2(\sigma^2 - a_{22}^2 - a_{23}a_{32} \\ &- a_{12}a_{21}) + \overline{D}_3(\sigma^2 - a_{33}^2 - a_{13}a_{31} - a_{23}a_{32}), \\ \beta_V &= (\overline{D}_1 + \overline{D}_3)(\overline{D}_2 + \overline{D}_3)(a_{11} + a_{22}) + (\overline{D}_1 + \overline{D}_2)(\overline{D}_2 + \overline{D}_3) \\ &\times (a_{11} + a_{33}) + (\overline{D}_1 + \overline{D}_2)(\overline{D}_1 + \overline{D}_3)(a_{22} + a_{33}), \\ \delta_V &= (\overline{D}_1 + \overline{D}_2)(\overline{D}_1 + \overline{D}_3)(\overline{D}_2 + \overline{D}_3). \end{aligned}$$

Again, to satisfy inequality (17) the sum of two coefficients on the main diagonal of matrix $\{a_{ij}\}$ must be greater than zero [17].

As we see, our diagonal coefficients a_{11}, a_{22} and a_{33} are negative for all values of the system parameters. This means that the catalytic CO oxidation reaction is not autocatalytic because, as was mentioned above, for autocatalytic reactions at least one of the diagonal coefficients must be greater than zero. Nevertheless, we show further that conditions of the existence of the Turing (16) and the Hopf (17) bifurcations can be satisfied in our non-autocatalytic system at certain values of the system parameters. We associate the emergence of these instabilities with an interaction of nonlinear local transformations with positive feedback (i.e. surface phase transitions) and transport processes (diffusion) which spatially coupling the system.

2. Results and discussion

2.1. Homogeneous surface

As was mentioned above, the system is stable if

$$\mathrm{Re}\,\omega(k) < 0 \quad \text{for} \quad \forall k, \tag{18}$$

that is when all normal modes are exponentially reduced. In the case when for at least one mode at a certain k inequality $\mathrm{Re}\,\omega(k) > 0$ becomes true, the whole system becomes unstable because the amplitude of the corresponding motion increases. The system can loss stability of the homogeneous state in two ways – either through the Hopf bifurcation leading to the temporal patterns formation (oscillations) in the system or through the Turing bifurcation that leads to the formation of regular spatial patterns.

Figure 1 shows the dispersion dependences of real $\mathrm{Re}\,\omega$ and imaginary $\mathrm{Im}\,\omega$ parts as functions of the wave number k for different values of the coefficient $\overline{D}_3$. Values of other model parameters used in our calculations are presented in Table 1.

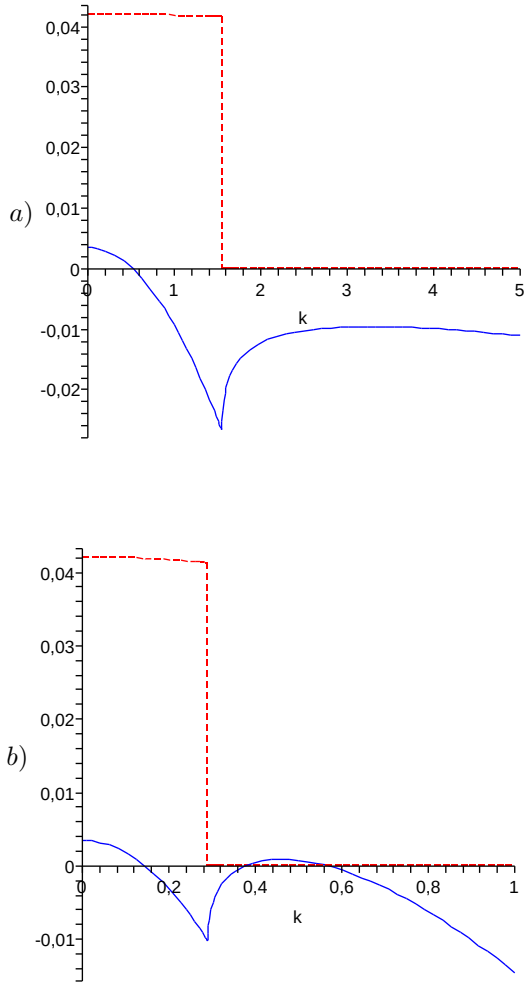

Figure 1. Dispersion dependences of real $\mathrm{Re}\,\omega$ (solid line) and imaginary $\mathrm{Im}\,\omega/10$ (dash line) parts on the wave number k for $\overline{D}_3 = 0.000175$ (a) and $\overline{D}_3 = 0.3$ (b), respectively. Diffusion coefficients $\overline{D}_1 = 0.035$, $\overline{D}_2 = 0.000035$ and partial pressure $\overline{p}_{\mathrm{CO}} = 0.06$ are the same in all cases.

At pressure $\overline{p}_{\mathrm{CO}} = 0.06$ the system is characterized by one stationary point ($\theta_{\mathrm{CO}} = 0.359$, $\theta_{\mathrm{O}} = 0.123$, $\theta_{1\times1} = 0.545$), and under such

values of the system parameters it is unstable, because $\mathrm{Re}\,\omega > 0$ at $k_0 = 0$. Hence, we have a realization of the Hopf bifurcation scenario with $\mathrm{Im}\,\omega(k_0) = 0.419$, $\mathrm{Re}\,\omega(k_0) = 0.003$ where $k_0 = 0$. As we know [13], the Hopf instability is the local dynamic instability arising in nonlinear systems with multiple time-scales, and requires the following conditions: $\mathrm{Im}\,\omega(k_0) \neq 0$, $\mathrm{Re}\,\omega(k_0) > 0$ where $k_0 = 0$. In the phase space of the system it causes a new attractor – a closed orbit called the limit cycle [1]. As a result of the Hopf bifurcation, evolution of the system takes place by the states of the limit cycle.

The corresponding phase portrait of the system is depicted in Figure 2. As we can see, the phase trajectory screwed on the closed curve – the limit cycle. Both average coverages of the adsorbates and the local fraction of the surface area found in the unreconstructed 1×1 structure undergo periodic oscillations arised because of the Hopf bifurcation. The instability of such type generates periodic in time patterns, i.e. waves.

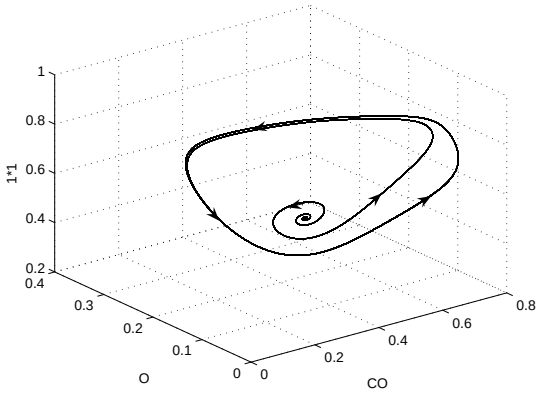

Figure 2. The limit cycle in the phase portrait of the system in autowave regime at pressure $\overline{p}_{\mathrm{CO}} = 0.06$.

A change of the diffusion coefficient $\overline{D}_3$ does not affect the stability of the system. However, as figure 1 depicts, depending on diffusion coefficient $\overline{D}_3$ the Turing instability can occur in the system. In contrast to the Hopf bifurcation, the Turing bifurcation is not dynamic. It is called bifurcation caused by the diffusion. The Turing bifurcation requires $\mathrm{Im}\,\omega(k_T) = 0$, $\mathrm{Re}\,\omega(k_T) > 0$ where $k_T > 0$ is a value of wave number k corresponding to the second peak of the curve $\mathrm{Re}\,\omega(k)$ [13]. As ones see from figure 1b, at a certain choice of the diffusion parameters of

the system, namely $\overline{D}_1 = 0.035$, $\overline{D}_2 = 0.000035$ and $\overline{D}_3 = 0.3$, condition $\mathrm{Im}\,\omega(k_T) = 0$, $\mathrm{Re}\,\omega(k_T) = 0.001 > 0$ becomes true for $k_T = 0.475$. It causes periodic in space and stationary in time concentration patterns called the Turing patterns.

Besides, we have tested whether analytical conditions (16) and (17) for the existence of the Turing and the Hopf bifurcations, respectively, are performed for a given set of the system parameters. We have built a plot of the function $d(k^2)$ which is shown in Figure 3. We have got that

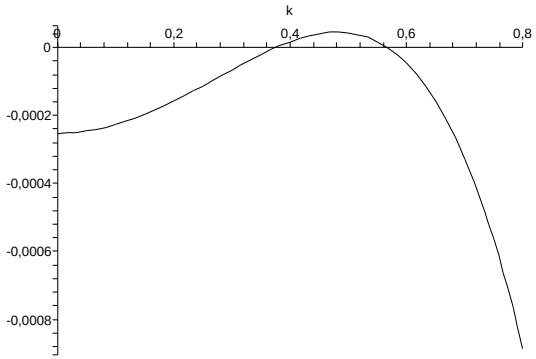

Figure 3. Dependence of the coefficient d of cubic equation (10) on the wave number k at pressure $\overline{p}_{\mathrm{CO}} = 0.06$.

the maximum of the curve lies in a region of positive values and is

$$d_{\max}(k_T^2) = 5 \cdot 10^{-5} > 0. \tag{19}$$

Analytical conditions (16) gives the same value of $d_{\max}(k_T^2)$. This means the appearance of one real positive eigenvalue in the system. Really, there are three real roots of cubic equation (10) for this set of the parameters. And one of them is positive: $\omega_1 = 0.001$, $\omega_2 = -0.069$, $\omega_3 = -0.724$. From analytical conditions (17) we have

$$F_{\max}(k_0^2) = 0.0037 > 0. \tag{20}$$

In this case we have two complex conjugate eigenvalues with positive real part: $\omega_{1,2} = 0.003 \pm 0.419i$, $\omega_3 = -0.725$. The first case corresponds to the Turing bifurcation, and the second – to the Hopf one.

2.2. Inhomogeneous surface

To investigate the effect of inhomogeneities on the surface, we consider an one-dimensional Pt(110) substrate of a size $L_x = 1$ μm with various surface phases – reconstructed central 1×2 phase surrounded by the unreconstructed 1×1 phase. Periodic boundary conditions were chosen assuming that there is no flow through the boundary of the interval [0,1]. The initial conditions were set as follows:

$$\theta_{\mathrm{CO}}(x, t=0) = \theta_{\mathrm{CO},s}, \tag{21}$$

$$\theta_{\mathrm{O}}(x, t=0) = \begin{cases} \theta_{\mathrm{O},s}, & x < 0.3 \quad \text{and} \quad x > 0.7, \\ 0, & 0.3 < x < 0.7, \end{cases} \tag{22}$$

$$\theta_{1\times1}(x, t=0) = \begin{cases} 1, & x < 0.3 \quad \text{and} \quad x > 0.7, \\ 0, & 0.3 < x < 0.7. \end{cases} \tag{23}$$

Parameters of the reaction and diffusion correspond to the homogeneous oscillating state. This means that in the case when the entire surface of the substrate had uniform structure, the temporal behavior would be characterized by homogeneous periodic oscillations of coverages $\theta_{\mathrm{CO}}(x,t) = \theta_{\mathrm{CO}}(t)$, $\theta_{\mathrm{O}}(x,t) = \theta_{\mathrm{O}}(t)$ and the local fraction of the surface area in the unreconstructed 1×1 phase $\theta_{1\times1}(x,t) = \theta_{1\times1}(t)$.

In the case when the reconstructed 1×2 phase is located inside the unreconstructed 1×1 phase, the gradients of the adsorbate coverages and of the surface geometry near the $1 \times 2/1 \times 1$-interfaces lead to the transition to a highly nonuniform state that, in turn, leads to a deformation of the wave front. To see this, in figure 4 we present the evolution of the adsorbate coverages θ_{CO}, θ_{O} and the substrate geometry $\theta_{1\times1}$ at pressure $\overline{p}_{\mathrm{CO}} = 0.06$. We observe the occurrence of periodic in space and time patterns for θ_{O} coverage. The distributions of θ_{CO} coverage and $\theta_{1\times1}$ surface geometry are almost homogeneous in space.

Figure 5 presents the spatial distribution of oxygen coverage θ_{O} at pressure $\overline{p}_{\mathrm{CO}} = 0.06$ at the moment t =2000. Coverage of adsorbed oxygen is sensitive to the surface structure at an initial moment, and the nonuniform distribution of oxygen sets on the surface with time. The oxygen distribution has oscillating behaviour, we see homogeneous periodic oscillations of θ_{O} coverage along the entire surface.

Figure 6 depicts the temporal evolution of oxygen coverage in the form of amplitude map. Figure 6*a* shows that at partial pressure $\overline{p}_{\mathrm{CO}} = 0.06$ an auto-oscillatory regime appears in the system when condition (17) of the existence of the Hopf bifurcation is satisfied. Figure 6*b* demonstrates that at pressure $\overline{p}_{\mathrm{CO}} = 0.053$ the system evolves to a steady state through the damped oscillations. As we see, a perturbation of the initial

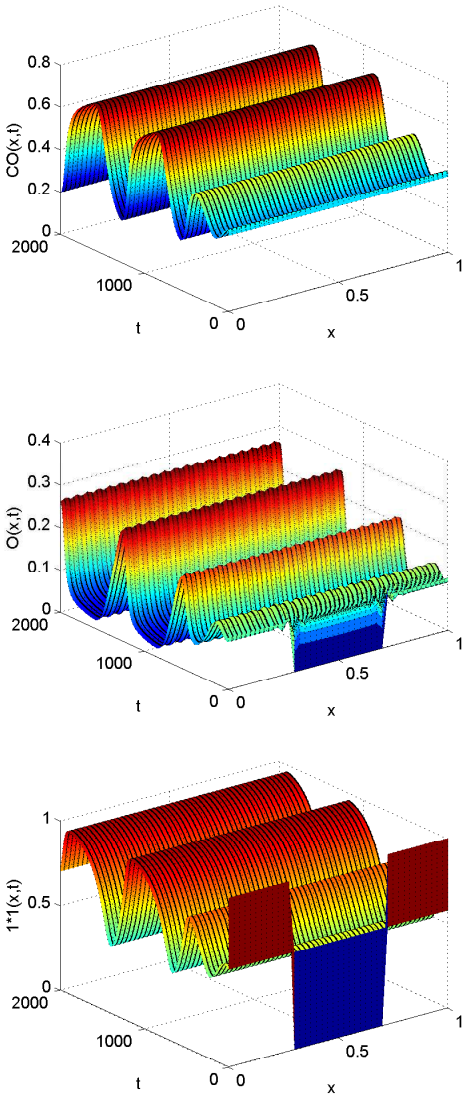

Figure 4. Oscillations of the adsorbate coverages θ_{CO}, θ_{O} and the surface geometry $\theta_{1\times1}$ at pressure $\overline{p}_{\mathrm{CO}} = 0.06$.

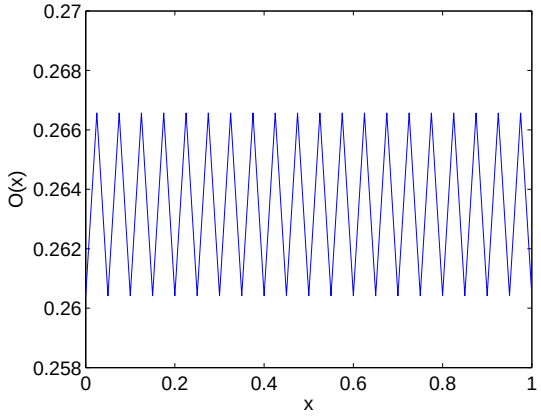

Figure 5. Spatial distribution of oxygen coverage θ_{O} at pressure $\overline{p}_{\mathrm{CO}} = 0.06$ at the moment t =2000.

spatial homogeneous distributions of oxygen coverage and surface geometry leads to the growth of the perturbations by the Turing mechanism and to the formation of regular spatiotemporal (figure 6*a*) and spatial (figure 6*b*) patterns with durable coexistence of regions with high and low oxygen concentrations on the surface.

Conclusions

The catalytic carbon monoxide oxidation reaction model taking diffusion processes on the Pt(110) surface into account has been considered. The dispersion dependences $\mathrm{Re}\,\omega$ and $\mathrm{Im}\,\omega$ on the wave number k have been built. Despite that the CO oxidation reaction is not autocatalytic, we have shown that the analytic conditions of the existence of the Turing and the Hopf bifurcations can be satisfied at certain values of the system parameters. Thus, the system may lose its stability in two ways – either through the Hopf bifurcation leading to the formation of temporal patterns in the system, namely oscillations, or through the Turing bifurcation leading to the formation of regular spatial patterns. At simultaneous implementation of both scenarios spatiotemporal patterns for oxygen coverage θ_{O} have been observed in the system. We associate the emergence of these instabilities with an interaction of nonlinear local transformations with positive feedback (i.e. surface phase transitions) and transport processes (diffusion) which spatially coupling the system.

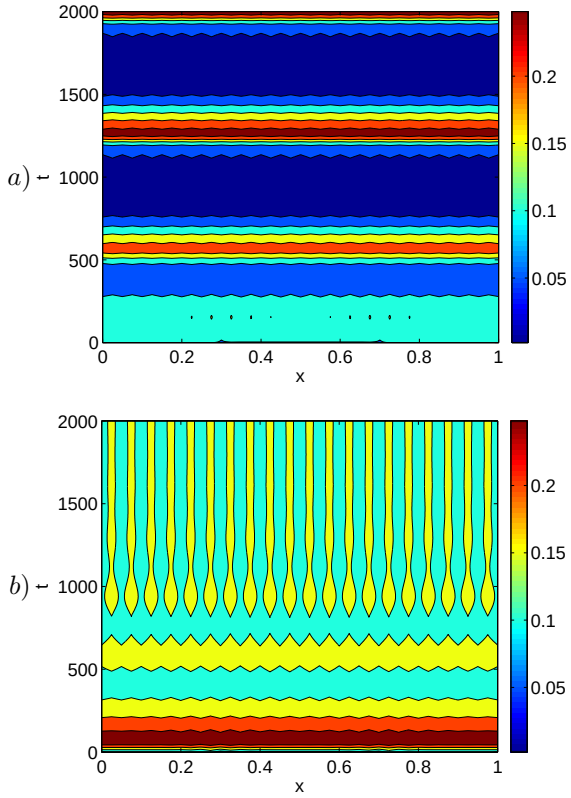

Figure 6. Amplitude map of oxygen coverage θ_{O} at pressures $\overline{p}_{\mathrm{CO}} = 0.06$ (a) and $\overline{p}_{\mathrm{CO}} = 0.053$ (b).

The distribution of θ_{CO} is almost homogeneous in space and independent of the surface geometry.

References

1. Ebeling W. Patterns formation in irreversible processes. – Moscow-Izhevsk, 2004 (in Russian).
2. Cross M., Greenside H. Pattern formation and dynamics in nonequilibrium systems. – New York, 2009.
3. Bertram M., Mikhailov A.S., Pattern formation in a surface chemical reaction with global delayed feedback // Phys. Rev. E. – 2001. – Vol. 63. – Pp. 066102-1-13.
4. Kharchenko V.O., Kharchenko D.O., Kokhan S.V., Vernyhora I.V. and Yanovsky V.V., Properties of nano-islands formation in nonequilibrium reaction-diffusion systems with memory effects // Phys. Scr. – 2012. – Vol. 86. – Pp. 055401-1-10.
5. Verdasca J., Borckmans P., Dewel G., Spatiotemporal patterns in CO oxidation on Pt(110): The role of nonlinear diffusion // Phys. Rev. E. – 2001. – Vol. 64, no. 5. – Pp. 055202-1-4.
6. Bertram M., Mikhailov A.S., Pattern formation on the edge of chaos: Mathematical modeling of CO oxidation on a Pt(110) surface under global delayed feedback // Phys. Rev. E. – 2003. – Vol. 67, no. 3. – Pp. 036207-1-11.
7. Hoyle R.B., Anghel A.T., Proctor M.R.E., King D.A., Pattern Formation during the Oxidation of CO on Pt(100): A Mesoscopic Model // Phys. Rev. Lett. – 2007. – Vol. 98, no. 22. – Pp. 226102-1-4.
8. Pavlenko N., CO-activator model for reconstructing Pt(100) surfaces: Local microstructures and chemical turbulence // Phys. Rev. E. – 2008. – Vol. 77, no. 2. – Pp. 026203-1-10.
9. Gorodetskii V.V., Drachsel W., Kinetic oscillations and surface waves in catalytic CO + O_2 reaction on Pt surface: Field electron microscope, field ion microscope and high resolution electron energy loss studies // Appl. Cat. A. – 1999. – Vol. 188, no. 1-2. – Pp. 267-275.
10. von Oertzen A., Rotermund H.H., Mikhailov A.S., and Ertl G., Standing Wave Patterns in the CO Oxidation Reaction on a Pt(110) Surface: Experiments and Modeling // J. Phys. Chem. B. – 2000. – Vol. 104. – P. 3155.
11. Bertram M., Beta C., Pollmann M., Mikhailov A.S., Rotermund H.H., and Ertl G., Pattern formation on the edge of chaos: Experiments with CO oxidation on a Pt(110) surface under global delayed feedback // Phys. Rev. E. – 2003. – Vol. 67. – Pp. 036208-1-9.
12. Gichan O.I., Lerman L.B., Grechko L.G., Sklyarov Yu.P., Spatiotemporal patterns in the FitzHugh-Nagumo model for excitable and bistable media. // Bulletin of Kiev university. Series: Physics & Mathematics. – 2005. – Vol. 1. – Pp. 311-318 (in Ukrainian).
13. Gichan O.I., Grechko L.G., Mixed modes of the FitzHugh-Nagumo model: interaction and competition of the Hopf and Turing instabilities. // Bulletin of University of Kyiv. Series: Physics & Mathematics. – 2007. – Vol. 4. – Pp. 311-315 (in Ukrainian).
14. Vanag V.K., Waves and patterns in reaction-diffusion systems.

Belousov-Zhabotinsky reaction in water-in-oil microemulsions // Physics-Uspekhi (Advances in Physical Sciences). – 2004. – Vol. 174, no 9. – P. 991 (in Russian).
15. Bzovska I.S., Mryglod I.M., Chemical oscillations in catalytic CO oxidation reaction // Condens. Matter Phys. – 2010. – Vol. 13, no. 3. – Pp. 34801-1-5.
16. Bzovska I.S., Mryglod I.M., Surface structures in a model of carbon monoxide oxidation reaction. - Lviv: Institute for condensed matter physics of NASU, 2015. - 15 p. - (Preprint / NAS of Ukraine. Institute for condensed matter physics; ICMP-15-02U) (in Ukrainian).
17. Borina M.U., Polezhaev A.A., Diffusion instability in a threevariable reaction-diffusion model // Computer Research and Modeling. – 2011. – Vol. 3, no. 2. – Pp. 135-146 (in Russian).

CONDENSED MATTER PHYSICS

The journal **Condensed Matter Physics** is founded in 1993 and published by Institute for Condensed Matter Physics of the National Academy of Sciences of Ukraine.

AIMS AND SCOPE: The journal **Condensed Matter Physics** contains research and review articles in the field of statistical mechanics and condensed matter theory. The main attention is paid to physics of solid, liquid and amorphous systems, phase equilibria and phase transitions, thermal, structural, electric, magnetic and optical properties of condensed matter. Condensed Matter Physics is published quarterly.

ABSTRACTED/INDEXED IN: Chemical Abstract Service, Current Contents/Physical, Chemical&Earth Sciences; ISI Science Citation Index-Expanded, ISI Alerting Services; INSPEC; "Referatyvnyj Zhurnal"; "Dzherelo".

CONTACT INFORMATION:
Institute for Condensed Matter Physics
of the National Academy of Sciences of Ukraine
1 Svientsitskii Str., 79011 Lviv, Ukraine
Tel: +38(032)2761978; Fax: +38(032)2761158
E-mail: cmp@icmp.lviv.ua http://www.icmp.lviv.ua